Structural Chemistry
https://doi.org/10.1007/s11224-020-01557-1

ORIGINAL RESEARCH

The study of thiazole adsorption upon BC_2N nanotube: DFT/TD-DFT investigation

Nafiseh Abdolahi[1] · Masoud Bezi Javan[2] · Konstantin P. Katin[3,4] · Alireza Soltani[1] · Shamim Shojaee[5] · Sara Kaveh[5]

Received: 30 January 2020 / Accepted: 8 May 2020

Abstract

Herein, we evaluated the adsorption of thiazole over the surface of BC_2N nanotube using PBE and M06-2X functionals and 6-311G** standard basis set. We considered one and two thiazole molecules over the outer sidewall of BC_2N nanotube. Furthermore, we found that the adsorption energy of thiazole (state **II**) from its nitrogen head on the boron atom of BC_2N nanotube is greater than other states (about − 0.90 eV by PBE and − 1.09 eV by M06-2X functional). It was found that the energy gap of BC_2N nanotube is significantly reduced from 0.61 to 0.25 eV after the thiazole adsorption (state **II**). Our results also indicated that the electronic and optical properties of BC_2N nanotube are significantly altered on the adsorption of thiazole.

Keywords BC_2N nanotube · Thiazole · Adsorption · Density functional theory · Electronic structure, Optical structure

Introduction

Thiazoles (C_3NH_3S) and their derivatives have been regularly discovered as a vital compound of novel and structurally various accepted products that reveal numerous biological behavior such as thiamine, penicillin G, amphetamine drugs, and vitamin B_1 which are served as an electron descend. They are used as systematic reagents and lively center in the study of important evolution of metals such as cadmium, lead, copper, and gold [1–3]. Thiazole coenzyme structure is most for decarboxylation of α-ketoacids [4]. Thiazole is a heterocyclic compound that contains anti-inflammation, anti-hypertension, antibacterial, and anti-human immunodeficiency virus effects [5–8]. In later years, significant efforts led to the creation of tube-like structures. The full substitute for carbon in the CNT construction, as a result of alternating boron and nitrogen atoms, leads to the configuration of boron nitride nanotubes (BNNTs) with relatively diverse electronic properties while compared with its carbon-based analog [9–15]. BN nanotubes are also semi-conductive with an energy gap of 5.5 eV [16, 17]. The electronic properties of nanostructure material can therefore be considerably adapted to the existence of defects, more than ever as substitution dopants are incorporated into the honeycomb structure [18–20]. In addition to BNNTs, other types of nanotubes such as B–C–N nanotubes have been synthesized by electrical arc discharge, pyrolysis, laser ablation, and other recently with laser vaporization, motivating a large number of theoretical investigations [21–27]. The BC_2N nanotube is well known as one of the most stable forms of the BCN layers based and nanotube class which shows acceptable features including low toxicity, high oxidative stability, and optoelectronic properties [28, 29]. In a theoretical study in 2003, Schmidt et al. showed that the beginning of substitution of C impurities in a BNNT structure induces an important decrease of the configuration energy when compared with other types of national defects [30]. Also, the first-principles calculations by Wu et al. showed that the substitution of C atoms can produce spontaneous magnetization [31]. Some time ago, B–C–N thin films with diverse chemical

✉ Alireza Soltani
Alireza.soltani46@yahoo.com; alireza.soltani@goums.ac.ir

1 Golestan Rheumatology Research Center, Golestan University of Medical Science, Gorgan, Iran

2 Department of Physics, Faculty of Sciences, Golestan University, Gorgan, Iran

3 Nanoengineering in Electronics, Spintronics and Photonics, Institute National Research Nuclear University "MEPhI", Kashirskoe Shosse 31, Moscow, Russia 115409

4 Laboratory of Computational Design of Nanostructures, Nanodevices, and Nanotechnologies, Research Institute for the Development of Scientific and Educational Potential of Youth Aviatorov str. 14/55, Moscow, Russia 119620

5 Department of Chemistry, Gorgan Branch, Islamic Azad University, Gorgan, Iran

Published online: 20 May 2020

compositions were organized by chemical steam deposition (CVD) using BCl_3, N_2, H_2, CCl_4, or still acetylene (C_2H_2) [32–34]. Peyghan et al. have theoretically studied the reactivity and electronic sensitivity of perfect, Al-doped, and double-antisite defect BC_2N nanotubes on the adsorption of HCN molecule by DFT calculations. They found that the B–B antisite defect can significantly reduce the energy gap of adsorbent than other states [35]. For instance, Noei and Peyghan [36] have shown that BC_2N nanotube is a promising material for the detection of formaldehyde. Baei and co-workers have found BC_2N nanotubes to be acceptable candidates for adsorption of Cl^- and F^- ions using DFT calculations [37]. Anafcheh and Ghafouri investigated the details of nitriloxide, azide, and azomethine adsorptions with BC_2N nanotube by M06-2X functional, and they have found that the values of interaction energies demonstrate the exothermic character of this study [38]. Thiazole and its derivatives as drug constituent(s) have great potential in a wide range of biological activities [39, 40]. On the other side, the thiazole ring is present in several anticancer drugs, such as thiazofurine, sulfathiazole, dasatinib, and bleomycin [41]. To our knowledge, a density functional theory (DFT) study of the interaction of thiazole with the surfaces of BC_2N nanotube (BC_2NNT) has not been reported. The main goal of this study surveys around the adsorption mechanism of thiazole on BC_2N nanotube. However, we expect that our studies can provide a better condition for thiazole adsorption upon the surface of BC_2N nanotube that may have the advantages with respect to its biocompatibility, solubility, and drug delivery.

Computational methods

In this research, the full geometry optimizations, optical structures, and electronic properties on the adsorption process of thiazole interacting with (6, 0) *zigzag* BC_2NNT were studied by using density functional theory (DFT) and time-dependent density functional theory (TD-DFT) calculations, where the ends of the BC_2NNT were saturated with hydrogen atoms. The influence of thiazole adsorption on BC_2NNT surfaces as a functional group and its effects on the electronic and optical properties of the nanotube were studied using the GAMESS program package [42]. All the atomic geometrical parameters of the structures were permitted to relax in the optimization at the DFT level within the generalized-gradient approximation functional with the Perdew-Burke-Ernzerhof (PBE) [43] and M06-2X functionals [45, 46] at the 6-311G** standard basis set [44]. To evaluate the accuracy of the PBE results, the PBE-D3 functional was also carried out to study the adsorption of thiazole on the BC_2N nanotube surface. Moreover, the time-dependent density functional theory (TD-DFT) has been carried out by the M06-2X and CAM-B3LYP in the gas phase regime [47]. To calculate total energies, the self-consistent field (SCF) convergence limit was set to 1.0×10^{-6} a.u. over energy and electron density. All calculations were fully optimized with the optimization criteria (max. force = 0.00045, RMS force = 0.0003, max. displacement = 0.0018, and RMS displacement = 0.0012). To study the interaction between the thiazole molecule and BC_2N nanotube, the adsorption energy (E_{ad}) was calculated using Eq. (1):

$$E_{ad} = E_{(Thiazole/BC2NNT)} - E_{(Thiazole)} - E_{(BC2NNT)} + BSSE \quad (1)$$

where $E_{(Thiazole/BC2NNT)}$ is the total energy of the complex consisting of thiazole molecule and BC_2N nanotube, while $E_{(Thiazole)}$ and $E_{(BC2NNT)}$ are the total energies of thiazole molecule and BC_2NNT, respectively. Basis set superposition error (BSSE) for the adsorption energies was corrected using the counterpoise method [48]. The values of HOMO energy (E_{HOMO}), LUMO energy (E_{LUMO}), energy gap (E_g), and Fermi level (E_{Fl}) parameters are calculated by the obtained results of the total density of state (TDOS) spectrum using GaussSum program [49]. The natural bond orbital (NBO) analysis was calculated at the same level of theory.

Result and discussion

Structural properties and adsorption energies

In this section, we discuss the structural properties containing the bond lengths and bond angles for the BC_2NNT and thiazole-attached (6, 0) BC_2NNT listed in Table 1. Figure 1 represented the structures of the optimized (6, 0) *zigzag* BC_2NNT and thiazole molecule. Based on PBE (B3LYP) functional, the length of C–S, C–N, and C=C bonds in the free thiazole is found to be 1.720 (1.734), 1.375 (1.378), and 1.361 (1.366) Å respectively. Abdel-Sattar et al. experimentally reported the length of C–S, C–N, and C=C bonds for the thiazole ring is 1.721, 1.379, and 1.321 Å [50]. Therefore, we

Table 1 Selected bond lengths and bond angles optimized of thiazole interacting with BC_2N nanotube

Nucleus	Base	I	PBE II	III	IV	V
Bond length (Å)						
B–C	1.539	1.545	1.606	1.547	1.551	1.603
N–C	1.430	1.425	1.407	1.420	1.418	1.405
B–N	1.452	1.451	1.532	1.539	1.541	1.549
C–C	1.371	1.370	1.370	1.370	1.363	1.371
Bond angle (°)						
C–B–N	118.33	118.38	110.10	118.36	110.63	110.15
B–C–B	110.84	110.81	116.60	110.82	115.77	116.32
B–N–C	122.46	122.40	123.71	122.48	123.79	122.53
C–C–B	116.21	116.17	116.11	116.19	117.46	116.13

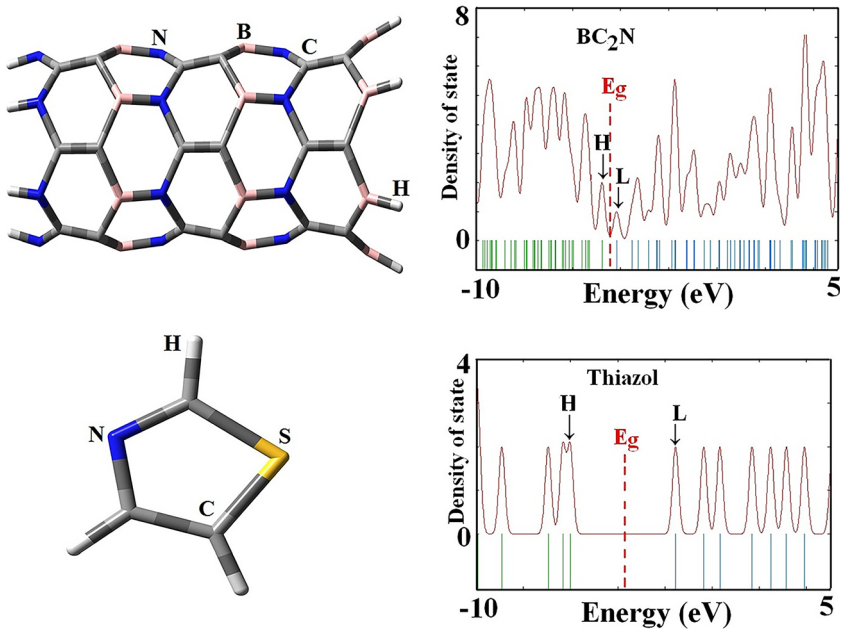

Fig. 1 Optimized structures of BC_2N nanotube and thiazole and their TDOS plots

have found that the PBE-D functional is more suitable (because of its closeness to the experimental data) than the B3LYP-D functional to recognize the accuracy of the geometry optimizations. After optimization, we studied the interaction of thiazole over the surface of BC_2N nanotube which leads to the changes in the average B–N bond lengths of the structure (see Fig. 2). For example, the average B–N bond length increased from 1.452 Å in the BC_2NNT to 1.541 Å in state **IV** (see Table 1). The length of B–N and B–C bonds was altered significantly from 1.452 and 1.539 Å by PBE functional and 1.439 and 1.540 Å by M06-2X functional in the free model to 1.532 and 1.606 Å by PBE and 1.531 and 1.601 Å by M06-2X functional in state **II**, which is in good agreement with the calculated results by Wand and co-workers [51]. The significant changes in the bond length of B–N in the thiazole-loaded BC_2NNT in states **II** and **V** are correlated to the covalent addition of thiazole on the BC_2NNT, leading to a change in hybridization from sp^2 to sp^3 at the B–N bond. Furthermore, the bond angle of the complexes, summarized in Table 1, indicates some difference in comparison with the perfect and thiazole-attached BC_2NNT complex in about five sites, reflecting various structural deformations. The different infrared (IR) vibration modes of the pure BC_2N nanotube is confirmed by B–N, C–N, and C–C at 1415, 1211, and 1693 cm^{-1}, respectively, showing the formation of BC_2N nanotube [52]. The IR spectra show the bands at 1495 and 1588 cm^{-1} assigned to skeletal vibrations of thiazole ring and the bands at 3242, 3273, and 3300 cm^{-1} corresponding to C–H stretching vibrations of the molecule. The band at 770 cm^{-1} is assigned to C–S stretching vibration [53]. The IR spectra of the thiazole-loaded BC_2NNT in state **II** show a medium to sharp band at 1496 cm^{-1} corresponding to ν(C=N) of the thiazole ring and the bands at 1419 and 1689 cm^{-1} assigned to B–N and C–C stretching vibrations [52]. The IR spectra of thiazole/BC_2NNT complex indicate medium to sharp bands within 1104–1175 cm^{-1} because of out-of-plane deformations of the aromatic C–H groups of the five-membered thiazole ring [54]. The enthalpy change (ΔH) and the Gibbs free energy change (ΔG) for state **II** as the most stable configuration were computed at 298.14 K and 1 atmosphere. Computed values of ΔG and ΔH in state II were − 0.29 and − 0.93 eV respectively. The calculated results again exhibit that the BC_2N nanotube has a strong interaction with the thiazole molecule to facilitate the recovery of the nanotube.

Negative values of the adsorption energy (exothermic) of thiazole molecule loaded to the BC_2NNT surface in the states **I** and **III** were − 0.13 and − 0.11 eV, respectively, proving to be an electrostatic interaction. Using the NBO analysis, no significant charge transfer (**I**, 0.014 |e|) takes place from molecule to tube, unlike state in **III**, a weak charge transfer (about 0.032 |e|) occurred from tube to molecule showing that the molecule acts an electron acceptor. In state **II**, the interaction of B atoms in the BC_2NNT improves the adsorption behavior of thiazole (from its N head). The corresponding computed adsorption energy and distance interaction values were found to be − 0.90 eV and 1.657 Å, respectively, indicating that this interaction is exothermic due to the negative partial charge on the nitrogen atom (− 0.366 e) of the molecule which makes it reactive over Lewis acid sites of boron atoms in the structure of nanotube. NBO charge reveals that about 0.277 |e| is transferred from the molecule to tube (**II**), indicating that the interaction between two species is covalent in nature. We consider the effect of dispersion correction energy at the DFT-D3 on the thiazole-BC_2NNT system. Each functional seems to

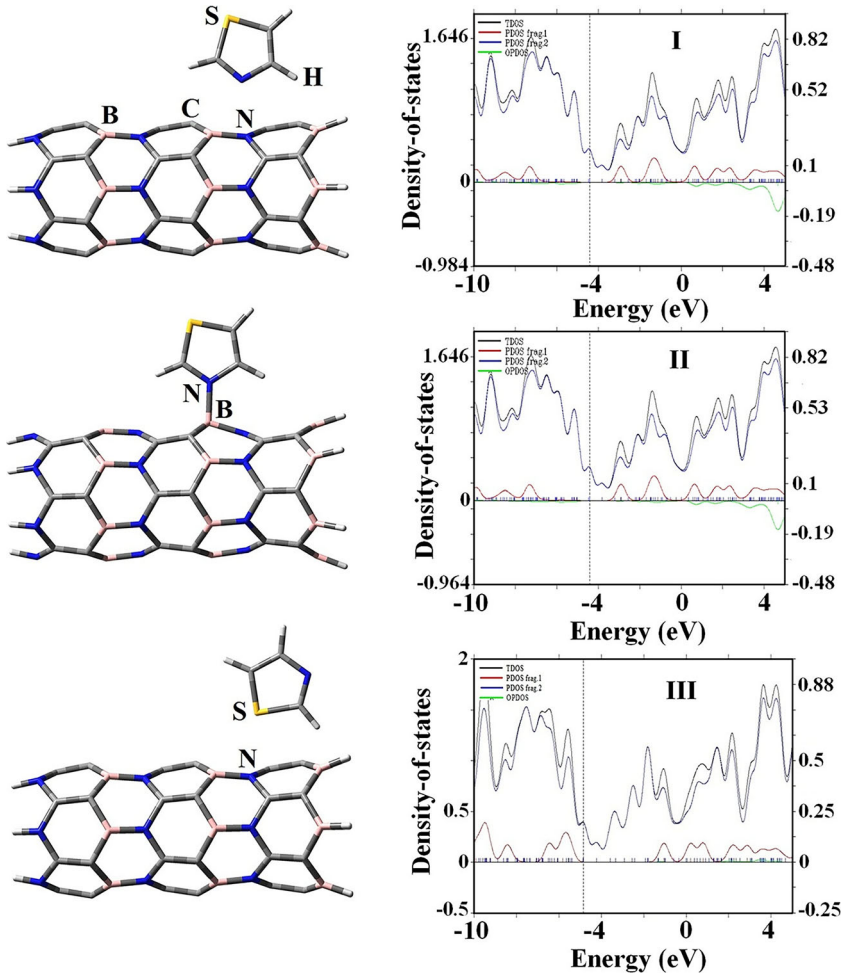

Fig. 2 The optimized geometries and their PDOS plots of BC_2N nanotubes interacting with thiazole molecule

generate the various behavior in the adsorption energy. The PBE-D3 functional predicts slightly higher energetic differences between the thiazole and BC_2NNT when compared with PBE. The PBE-D3 functional in the most stable state (**II**) can change E_{ad} by as much as 0.3 eV on the thiazole-BC_2NNT system. The computed E_{ad} and charge which is transferred for the thiazole to the BC_2NNT are about − 0.99 eV and 0.255 |e| respectively by the PBE-D3 functional, suggesting a strong interaction. In contrast to PBE functional, when two thiazole molecules are attached to the same boron atom of BC_2NNT surface (**V**), the values of adsorption energy and the distance interaction are changed to − 1.0 eV and 1.625 Å. Politzer et al. previously showed that boron atoms are reactive to the electron-rich N atom of thiazole [55]. For the most stable configurations, the adsorption energy and distance interaction of thiazole on the BC_2NNT surface were calculated to be − 1.09 eV and 1.647 Å in state **II** and − 0.58 eV and 1.648 Å in state **V** by M06-2X functional, indicating a higher tendency for adsorption while also indicating an increase in the interaction distance when compared with the PBE functional. The M06-2X and PBE-D3 functionals show a little difference in the prediction of absorption energy between the thiazole and BC_2NNT. Moradi et al. investigated the interaction between thiazole and BNNT in the gas and solvent phases. Their calculations indicate that the values of adsorption energy for the thiazole over BNNT were − 0.34 and − 0.56 eV, while about 0.04 and 0.06 electrons were transferred from the thiazole to the nanotube in the gas and solvent phases, respectively [38]. However, the charge transfer and adsorption energy of I, III, and IV states indicate non-covalent interaction between thiazole molecule and BC_2N nanotube, as presented in Table 2. In contrast, the adsorption energy of thiazole on the outer wall of BP nanotube [2] is about − 0.22 eV by B3LYP method after the use of basis set superposition errors (BSSE). The average adsorption energy per molecule in states **IV** and **V** was equal to − 0.27 and − 0.41 eV per molecule (see Table 2), respectively. While this is high, it corroborates that the thiazole molecule in state **V** could be stabilized from its N head over the B atom of the tube (see Fig. 3). The adsorption energy value of hydrogen fluoride (HF) upon the exterior wall of BC_2N nanotube was calculated to be − 1.0 eV using B3LYP functional by Peyghan and Noei [34]. In the most stable state (**V**), it is comprehensible that the dipole moment value of BC_2NNT is reduced with an increase

Table 2 Adsorption energy (E_{ad}), highest occupied molecular orbital (HOMO), lowest unoccupied molecular orbital (LUMO), energy gap (E_g) energy, Fermi level (E_{Fl}), and dipole moment (DM) of thiazole adsorbed on BC_2NNT surfaces by PBE functional

Parameters	Thiazole	Base	I	II	III	IV	V
E_{ad} (eV)	-	-	− 0.13	− 0.90	− 0.11	− 0.27	− 0.41
HOMO (eV)	− 6.02	− 4.78	− 3.82	− 4.48	− 4.23	− 2.02	− 2.20
LUMO (eV)	− 1.55	− 4.17	− 4.42	− 4.23	− 4.85	− 1.70	− 1.90
E_g (eV)	4.47	0.61	0.60	0.25	0.62	0.32	0.30
ΔE_g (%)	-	-	1.64	59.01	3.28	47.54	50.82
E_{Fl} (eV)	− 3.79	− 4.48	− 4.12	− 4.53	− 4.54	− 4.41	− 4.10
DM (Debye)	1.36	28.16	27.50	27.94	29.83	26.49	25.51

in adsorption energy. The total dipole moment value of BC_2N nanotube was equal to 28.16 Debye ($X = -1.4826$, $Y = 0.0$, $Z = -28.1264$) and thus it decreases to 25.51 Debye in state **V** ($X = -1.0737$, $Y = 0.0125$, $Z = -25.4924$). Nevertheless, because of the molecule asymmetry, the dipole structure along the BC_2N nanotube axis (here, the Z-axis) reveals the same behavior as the adsorption energy and more alters according to the molecular orientation (state **V**), while the change of total dipole moment in the state **II** is different ($X = -8.9131$, $Y = -0.0001$, $Z = -26.4850$).

Our results represent negative adsorption energy values for complexes **II** and **V** that is chemical functionalization of the adsorbed molecule to BC_2N nanotube surface, while for the other complexes, it is physisorption in nature. In Fig. 4, we depicted the electron charge density distribution around BC_2N interacting with thiazole molecule in state **II** of the considered configurations. Clearly depicted in Fig. 4, the charge density is localized around the separated interacting systems and there is significant overlapped charge density under the covalent interaction scheme leading to the chemical adsorption and high binding energy of the thiazole to the BC_2N nanotube. In Fig. 5, we show a map of total electron density (TED) that can be used to confirm our calculations based on the chemical strong bonding of thiazole in the interaction with BC_2N nanotube in states **II** and **V**. TED plot in states **II** and **V** indicate that an efficient charge transfer occurs between the thiazole and the BC_2N nanotubes.

The highest occupied molecular orbital (HOMO) and lowest unoccupied molecular orbital (LUMO) in the BC_2N nanotube and thiazole-attached BC_2N nanotube model were studied and summarized in Table 2. According to TDOS spectrum, the values of HOMO energy were changed from − 4.78 eV (base) to − 3.82 (**I**), − 4.48 (**II**), − 4.23 (**III**), − 2.02 (**IV**), and − 2.20 eV (**V**), and simultaneously the energies of LUMO were altered from − 4.17 eV (base) to − 4.42 (**I**), − 4.23 (**II**), − 4.85 (**III**), − 1.70 (**IV**), and − 1.90 eV (**V**). Energies of HOMO and LUMO of *zigzag* BC_2N nanotube was about − 5.41 and − 2.84 eV with the Fermi level (E_{Fl})

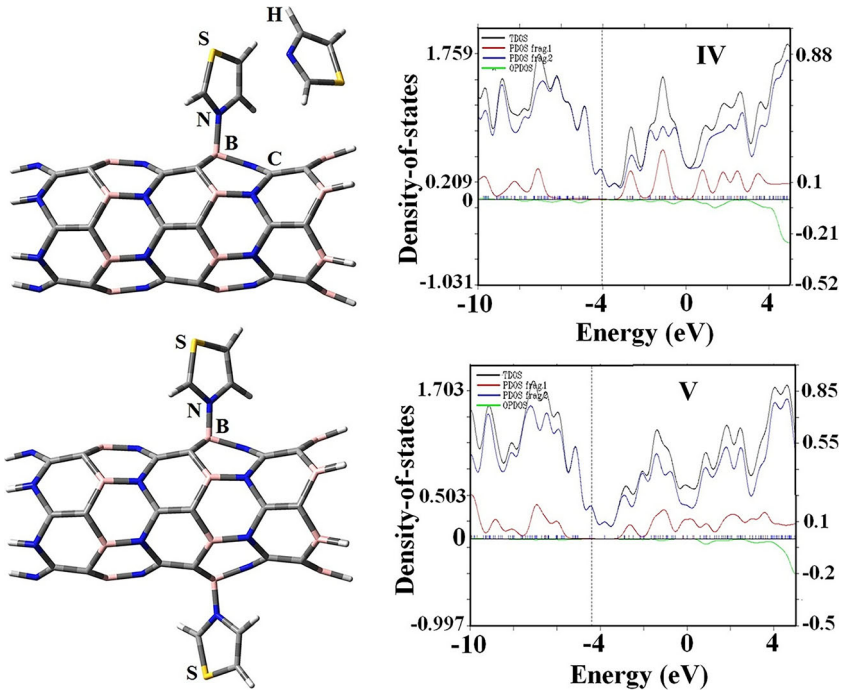

Fig. 3 The optimized geometries and their PDOS plots of BC_2N nanotubes interacting with two thiazole molecules

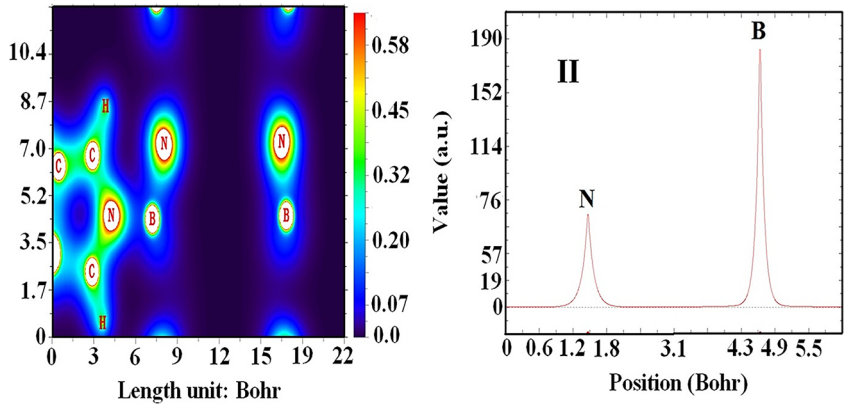

Fig. 4 Calculated the electron charge density of BC_2N nanotube interacting with thiazole molecule

of − 4.48 eV by the B3LYP method, which agrees with other theoretical reported values [33, 56, 57]. Energies of HOMO and LUMO were increased to − 6.76 and − 2.64 eV by M06-2X functional, respectively, whereas the value of E_{Fl} was about − 4.70 eV. Based on frontier molecular orbital (FMO), the HOMO and LUMO orbitals in the most stable states are more located near the B, N, and C atoms of the nanotube and the nitrogen atom of the molecule as presented in Fig. 6. The E_g value of BC_2N nanotube was found to be about 0.61 eV by PBE functional, which is close to the obtained reports by Soltani, Nejati, and Azevedo [57–59]. Based on the TDOS spectrum, the value of the E_g in state **II** is drastically reduced to 0.25 eV due to the thiazole adsorption on the outer surface of the tube, which leads to the hybridization of the π orbitals which is more considerable for vast deformation. Hence, the HOMO state is responsible for the decrement of E_g in comparison with the LUMO state. This lowering of E_g with the adsorption of thiazole may be able to enhance the reactivity of the system and result in charge transfer to happen between the molecule and BC_2NNT surface. The total density of state and projected density of state (PDOS) plots of the adsorption of thiazole on BC_2N nanotubes are presented in Figs. 2 and 3. The vertical lines show the Fermi level and the edge of the valence band. As shown in Fig. 6, state **II** has a significant reduction in the E_g of the BC_2N nanotube. Different structures of the PDOS indicate the dependency on the electronic structure of the system to the adsorption position and configuration of the thiazole interaction with BC_2N nanotube. Also, in all considered system, the overlap population density of state (OPDOS) shows the anti-bonding interaction of thiazole with BC_2N nanotube.

Optical properties of BC_2N nanotube and thiazole

TD-DFT calculations were carried out to study the optical band gap (E) and excitation wavelengths (λ_{max}) for BC_2N nanotube interacting with thiazole at M06-2X and CAM-B3LYP functionals and 6-311G** basis set [60, 61]. The oscillator strength (f) suggests the strength of the absorption and the H and L refer to the HOMO and LUMO states, respectively. The computed UV-vis spectra for BC_2N nanotube demonstrate two optical energy gap at 3.03 and 3.46 eV and show two excited states with the wavelengths of 358 and 408 nm, which are attributed to the inter-π band transitions [57, 61, 62]. The thiazole molecule indicates two maximum bands around λ_{max} = 223 nm (f, 0.008) and 203 nm (f, 0.086) by the M06-2X functional. Compared with M06-2X functional, the maximum bands at 221 nm (f, 0.007) and 207 nm (f, 0.086) are observed at the CAM-B3LYP functional. The adsorption of thiazole on the outer surface of BC_2N nanotube

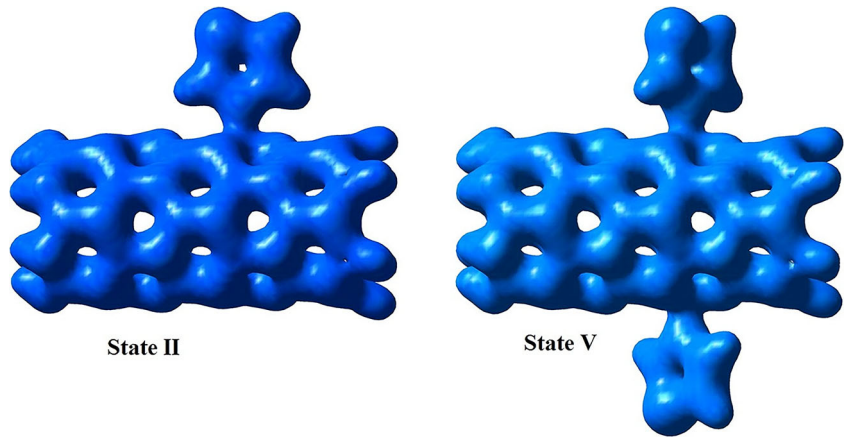

Fig. 5 Calculated the total density (ED) of BC_2N nanotube interacting with thiazole molecule

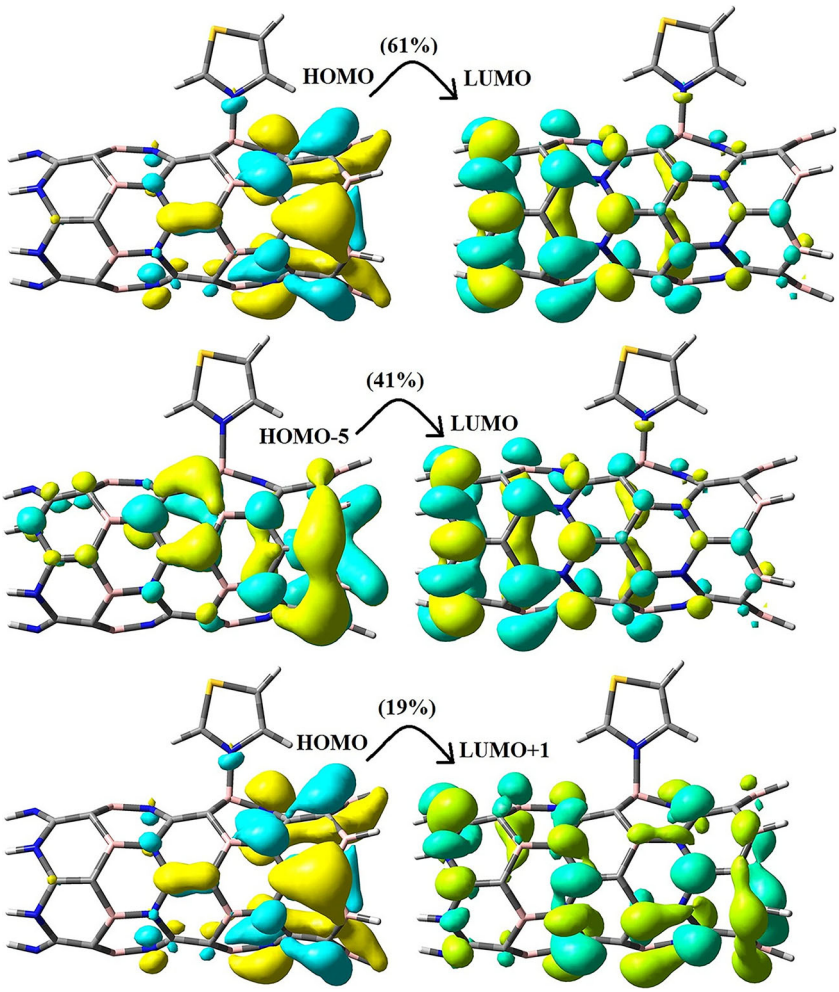

Fig. 6 HOMO and LUMO orbitals of the interaction of BC_2N with thiazole molecule (**II**)

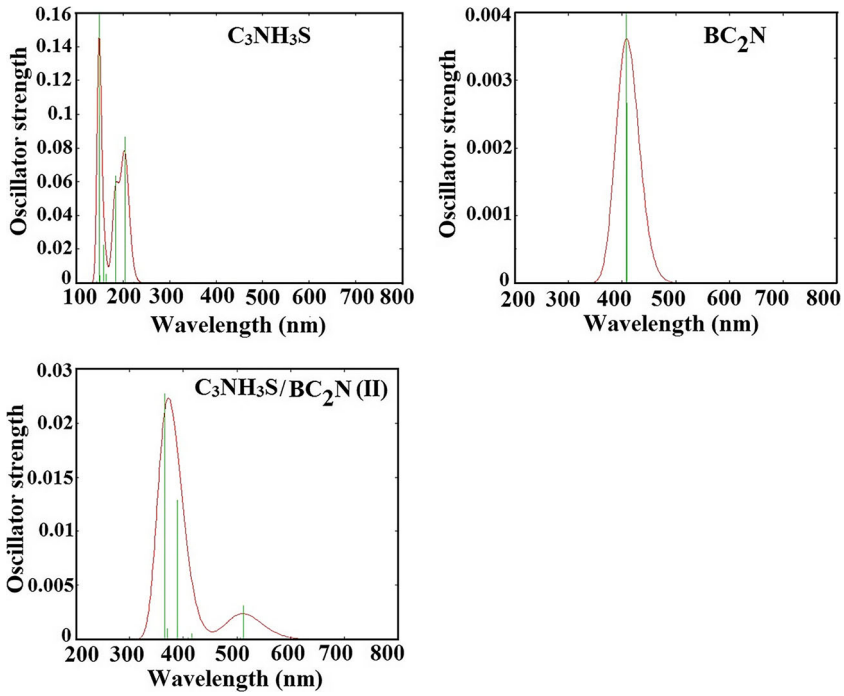

Fig. 7 Uv-vis spectrum of the structures

indicated some changes in the optical absorption spectra of this considered complex (see Fig. 7). In the TD-DFT calculation, an observed change of λ_{max} to a longer wavelength was attributed to the bathochromic effect (redshift in state **II**) with a narrow wavelength band at 365 nm (*f*, 0.023) corresponding to a HOMO→L + 1 (19%) transition (see Fig. 6) and an optical band gap of 3.39 eV by the M06-2X functional [57]. Two very weak bands observed (see state **II**) around 389 nm (*f*, 0.013) and 511 nm (*f*, 0.004) correspond to HOMO-5 → L (41%) and HOMO→L (61%) transitions with optical band gaps of 3.19 and 2.42 eV, respectively. In contrast with the M06-2X functional, we observed two maximum bands at 319 nm (*f*, 0.052) and 360 nm (*f*, 0.017) corresponding to HOMO→L + 3 (16%) and HOMO→L + 3 (20%) transitions and an optical band gaps of 3.87 and 3.44 eV by the CAM-B3LYP functional, respectively.

Conclusions

Density functional theory (DFT) and time-dependent density functional theory (TD-DFT) computations were carried out to illustrate adsorption properties of thiazole molecule toward BC_2N nanotube. Calculation results indicated that the only chemisorption can be taken place between thiazole and the outer surface of BC_2N nanotube (state **II**), while physisorption can happen in the other studied states. Using DFT calculations, we found the thiazole adsorption on BC_2N nanotube (state **II**) can significantly change the energy gap (ΔE_g = 59%) of an adsorbent. We have also found that the adsorption energy in state **II** increases with respect to other states as the Fermi level decreased a bit. The interaction between the thiazole and the BC_2N nanotube surface showed some changes in the optical absorption spectra of the complex. The study demonstrates various optoelectronic and charges transfer properties related to the orientation of thiazole on the BC_2NNT surface.

Acknowledgments We would like to thank the clinical Research Development Unit (CRDU), Sayad Shirazi Hospital, Golestan University of Medical Sciences, Gorgan, Iran.

Compliance with ethical standards

Conflict of interest The authors declare that they have no conflict of interest.

References

1. Pozharzskii AF, Soldatenkov AT, Katritzky AR (1997) Heterocycles in life and society. Chichester, Wiley
2. Sayyad-Alangi SZ, Baei MT, Hashemian S (2013) Adsorption and electronic structure study of thiazole on the (6,0) zigzag single-walled boron phosphide nanotube. J Sul Chem 34:407–420
3. Soleymani R, Salehi YM, Yousefzad T, Karimi-Cheshmeh Ali M (2012). Orient J Chem 28:627–638
4. Eicher T, Hauptmann S (2003) The chemistry of heterocycles2nd edn. Wiley-VCH, Weinheim, pp 149–184
5. Ayati A, Emami S, Asadipour A, Shafiee A, Foroumadi A (2015) Recent applications of 1,3-thiazole core structure in the identification of new lead compounds and drug discovery Eur. J Med Chem 97:699–718
6. Lu Y, Li C-M, Wang Z, Ross CR, Chen J, Dalton JT, Li W, Miller DD (2009) Discovery of 4-substituted methoxybenzoyl-aryl-thiazole as novel anticancer agents: synthesis, biological evaluation, and structure− activity relationships. J Med Chem 52:1701–1711
7. Liu W, Zhou J, Qi F, Bensdorf K, Li Z, Zhang H, Qian H, Huang W, Cai X, Cao P, Wellner A, Gust R (2011) Arch. Synthesis and biological activities of 2-amino-thiazole-5-carboxylic acid phenylamide derivatives, Pharm. Chem. Life Sci 344:451–458
8. Romagnoli R, Baraldi PG, Brancale A, Ricci A, Hamel E, Bortolozzi R, Basso G, Viola G (2011) Convergent synthesis and biological evaluation of 2-amino-4-(3′,4′,5′-trimethoxyphenyl)-5-aryl thiazoles as microtubule targeting agents. J Med Chem 54: 5144–5153
9. Iijima S (1991) Helical microtubules of graphitic carbon. Nature 354:56–58
10. Baei MT, Kanani Y, Joveini Rezaei V, Soltani A (2014) Adsorption phenomena of gas molecules upon Ga-doped BN nanotubes: a DFT study. Appl Surf Sci 295:18–25
11. Soltani A, Ghafouri Raz S, Joveini Rezaei V, Dehno Khalaji A, Savar M (2012) Ab initio investigation of Al- and Ga-doped single-walled boron nitride nanotubes as ammonia sensor. Appl Surf Sci 263:619–625
12. Duverger E, Gharbi T, Delabrousse E, Picaud F (2014) P Quantum study of boron nitride nanotubes functionalized with anticancer molecules. Phys Chem Chem Phys 16:18425–18432
13. Darwish AA, Fadlallah MM, Badawi A, Maarouf AA (2016) Adsorption of sugars on Al-and Ga-doped boron nitride surfaces: a computational study. Appl Surf Sci 377:9–16
14. Rodriguez Juarez A, Chigo Anota E, Hernandez Cocoletzi H, Riveros AF (2013) Adsorption of chitosan on BN nanotubes: a DFT investigation. Appl Surf Sci 268:259–264
15. Najafi Chermahini A, Teimouri A, Farrokhpour H (2014) Theoretical studies of urea adsorption on single wall boron-nitride nanotubes. Appl Surf Sci 320:231–236
16. Rubio A, Corkill JL, Cohen ML (1994) Theory of graphitic boron nitride nanotubes. Phys Rev B 49:5081–5084
17. Chopra NG, Luyken RJ, Cherrey K, Crespi VH, Cohen ML, Louie SG, Zettl A (1995) Boron nitride nanotubes. Science 269:966–967
18. Deng Z-Y, Zhang J-M, Xu K-W (2015) First-principles study of SO_2 molecule adsorption on the pristine and Mn-doped boron nitride nanotubes. Appl Surf Sci 347:485–490
19. Soltani A, Baei MT, Tazikeh Lemeski E, Kaveh S, Balakheyli H (2015) A DFT study of 5-fluorouracil adsorption on the pure and doped BN nanotubes. J Phys Chem Solids 86:57–64
20. Soltani A, Bezi Javan M (2015) Carbon monoxide interactions with pure and doped $B_{11}XN_{12}$ (X = Mg, Ge, Ga) nano-clusters: a theoretical study. RSC Adv 5:90621–90631
21. Muramatsu Y, Motoyama M, Utsumi W, Gullikson EM, Perera RCC (2002) Theoretically predicted soft x-ray emission and absorption spectra of graphitic-structured BC_2N. Adv Quantum Chem 42:353–361
22. Weng-Sieh Z, Cherrey K, Chopra NG, Blase X, Miyamoto Y, Rubio A et al (1995) Synthesis of $B_xC_yN_z$ nanotubules. Phys Rev B 15:11229–11233
23. Golberg D, Bando Y, Dorozhkin P, Dong ZC (2004) Synthesis, analysis and electrical property measurements of compounds nanotubes in the ceramic B-C-N system. MRS Bull 29:38–42

24. Zhang Y, Gu H, Suenaga K, Iijima S (1997) Heterogeneous growth of BCN nanotubes by laser ablation. Chem Phys Lett 279:264–269
25. Blase X, Charlier J-C, De Vita A, Car R (1999) Structural and electronic properties of composite BxCyNz nanotubes and heterojunctions. Appl Phys A Mater Sci Process 68:293–300
26. Ma RZ, Golberg D, Bando Y, Sasaki T (2004) Raman spectroscopy of graphite. Phil Trans R Soc Lond 362:2161–2186
27. Wang WL, Bai XD, Liu KH, Xu Z, Golberg D, Bando Y et al (2006) Direct synthesis of B-C-N single-walled nanotubes by bias-assisted hot filament chemical vapor deposition. J Am Chem Soc 128:6530–6531
28. Sivaprakash K, Induja M, Gomathi Priya P (2018) Facile synthesis of metal free non-toxic boron carbon nitride nanosheets with strong photocatalytic behavior for degradation of industrial dyes. Mater Res Bull 100:313–321
29. Lei W, Portehault D, Dimova R, Antonietti M (2011) Boron carbon nitride nanostructures from salt melts: tunable water-soluble phosphors. J Am Chem Soc 133(18):7121–7127
30. Schmidt TM, Baierle RJ, Piquini P, Fazzio A (2003) Theoretical study of native defects in BN nanotubes. Phys Rev B 67:113407
31. Wu J, Han W-Q, Walukiewicz W, Ager J-W, Shan W, Haller EE, Zettl A (2004) Raman spectroscopy and time-resolved photoluminescence of BN and $B_xC_yN_z$ nanotubes. Nano Lett 4: 647–650
32. Garel J, Zhao C, Popovitz-Biro R, Golberg D, Wang W, Joselevich E (2014) BCN nanotubes as highly sensitive torsional electromechanical transducers. Nano Lett 14:6132–6137
33. Kouvetakis J, Sasaki T, Shen C, Hagiwara R, Lerner M, Krishnan M, Bartlett N (1989) Novel aspects of graphite intercalation by fluorine and fluorides and new B/C, C/N and B/C/N materials based on the graphite network. Synth Met 34:1
34. Yin L-W, Bando Y, Golberg D, Gloter A, Li M-S, Yuan X, Sekiguchi T (2005) Porous BCN nanotubular fibers: growth and spatially resolved cathodoluminescence. J Am Chem Soc 127: 16354–16355
35. Ahmadi Peyghan A, Hadipour NL, Bagheri Z (2013) Effects of Al-doping and double-antisite defect on the adsorption of HCN on a BC_2N nanotube: DFT studies. J Phys Chem C 117:2427–2432
36. Ahmadi Peyghan A, Noei M (2014) Hydrogen fluoride on the pristine, Al and Si doped BC_2N nanotubes: a computational study. Comput Mater Sci 82:197–201
37. Baei MT, Ahmadi Peyghan A, Bagheri Z (2013) Selective adsorption behavior of BC_2N nanotubes toward fluoride and chloride. Solid State Commun 159:8–12
38. Anafcheh M, Ghafouri R (2014) 1,3-Dipolar cycloaddition of BC_2N nanotubes: a DFT study. Comput Theor Chem 1034:32–37
39. Theophil E, Siegfried H (2003) The chemistry of heterocycles structure: reactions, syntheses, and applications2nd edn. Wiley-VCH, Verlag GmbH, and Co., Weinheim
40. Dawane BS, Konda SG, Kamble VT, Chavan SA, Bhosale RB, Shaikh BM (2009) Multicomponent one-pot synthesis of substituted hantzsch thiazole derivatives under solvent free conditions. E J Chem 6:S358–S362
41. Ramos-Inza S, Aydillo C, Sanmartín C, Plano D (2019) Thiazole moiety: an interesting scaffold for developing new antitumoral compounds. https://doi.org/10.5772/intechopen.82741
42. Schmidt MW, Baldridge KK, Boatz JA, Elbert ST, Gordon MS, Jensen JH, Koseki S, Matsunaga N (1993). J Comput Chem 11: 1347
43. Wang Y, Perdew JP (1991) Correlation hole of the spin-polarized electron gas, with exact small-wave-vector and high-density scaling. Phys Rev B 44:13298
44. Foster JP, Weinhold F (1980) Natural hybrid orbitals. J Am Chem Soc 102:7211–7218
45. Zhao Y, Schultz NE, Truhlar GD (2006) Design of density functionals by combining the method of constraint satisfaction with parametrization for thermochemistry thermochemical kinetics, and noncovalent interactions. J Chem Theory Comput 2:364–382
46. Xu Z, Meher BR, Eustache D, Wang Y (2014) Insight into the interaction between DNA bases and defective graphenes: covalent or non-covalent. J Mol Graph Model 47:8–17
47. Bezi Javan M, Soltani A, Azmoodeh Z, Abdolahi N, Gholami N (2016) A DFT study on the interaction between 5-fluorouracil and $B_{12}N_{12}$ nanocluster. RSC Adv 6:104513–104521
48. Boys SF, Bernardi F (1970) The calculation of small molecular interactions by the differences of separate total energies. Some procedures with reduced errors. Mol Phys 19:553–566
49. O'boyle NM, Tenderholt AL, Langner KM (2008) Cclib: a library for package independent computational chemistry algorithms. J Comput Chem 29:839–845
50. Nour E, Abdel-Sattar A, El-Naggar AM, Abdel-Mottaleb MSA (2017) Novel thiazole derivatives of medicinal potential: synthesis and modeling. J Chem 2017:1–11
51. Wang Y, Zhou B, Yao X, Huang G, Zhang J, Shao Q (2014) Novel structure and abnormal electronic properties of ultra-thin BC2N nanotubes from first-principles investigation. Chem Phys Lett 616-617:61–66
52. Tripathi N, Yamashita M, Uchida T, Akai T (2014) Observations on size confinement effect in B-C-N nanoparticles embedded in mesoporous silica channels. Appl Phys Lett 105:014106
53. Issa RM, Khedr AM, Rizk H (2008) ^{1}H NMR, IR and UV/VIS spectroscopic studies of some Schiff bases derived from 2-aminobenzothiazole and 2-amino-3-hydroxypyridine. J Chin Chem Soc 55:875–884
54. Taurins A (1957) thiazoles: iii. infrared spectra of methylthiazoles. Can J Chem 35:423–427
55. Brez-Pei JP, Gonzzlez-Dsvila M (1988) Vibrational spectra of thiazole-2-carboxylic acid and thiazole-2-carboxylate ion. Spectrosc Lett 21(8):795–807
56. Varasteh Moradi A, Ahmadi Peyghan A, Hashemian S, Baei MT (2012) Theoretical study of thiazole adsorption on the (6,0) zigzag single-walled boron nitride nanotube. Bull Kor Chem Soc 33: 3285–3292
57. Soltani A, Azmoodeh Z, Bezi Javand M, Tazikeh Lemeskie E, Karami L (2016) A DFT study of adsorption of glycine onto the surface of BC_2N nanotube. Appl Surf Sci 384:230–236
58. Nejati K, Vessally E, Kheirollahi Nezhad PD, Mofid H, Bekhradnia A (2017) The electronic response of pristine, Al and Si doped BC_2N nanotubes to a cathinone molecule: computational study. J Phys Chem Solids 111:238–244
59. Azevedo S, Rosas A, Machado M, Kaschny JR, Chacham H (2013) Effects of deformation on the electronic properties of B–C–N nanotubes. J Solid State Chem 197:254–260
60. Abdolahi N, Aghaei M, Soltani A, Azmoodeh Z, Balakheyli H, Heidari F (2018) Adsorption of celecoxib on $B_{12}N_{12}$ fullerene: spectroscopic and DFT/TD-DFT study. Spectrochim Acta A Mol Biomol Spectrosc 204:348–353
61. Jeffrey JR, Kobayashi ASR, Ford MJ (2018) Understanding and calibrating density-functional-theory calculations describing the energy and spectroscopy of defect sites in hexagonal boron nitride. J Chem Theory Comput 14(3):1602–1613
62. Li H, Logoa O, Tay RY, Tsang SH, Jing L, Zhua M, Leong FN, Teo EHT (2017) Composition-controlled synthesis and tunable optical properties of ternary boron carbonitride nanotubes. RSC Adv 7:12511–12517